Tetrahedron Letters 54 (2013) 3630–3634

Contents lists available at SciVerse ScienceDirect

Tetrahedron Letters

journal homepage: www.elsevier.com/locate/tetlet

A novel rhodamine-based colorimetric chemodosimeter for the rapid detection of Al^{3+} in aqueous methanol: fluorescent 'OFF–ON' mechanism

Anamika Dhara [a], Atanu Jana [a], Saugata Konar [a], Sumanta Kumar Ghatak [a], Sangita Ray [a], Kinsuk Das [b], Anasuya Bandyopadhyay [a], Nikhil Guchhait [a], Susanta K. Kar [*,a]

[a] Department of Chemistry, University College of Science, University of Calcutta, 92, A.P.C. Road, Kolkata 700 009, India
[b] Department of Chemistry, Haldia Government College, Debhog Purba Midnapur 721 657, India

ARTICLE INFO

Article history:
Received 19 January 2013
Revised 23 April 2013
Accepted 28 April 2013
Available online 9 May 2013

ABSTRACT

A novel rhodamine-based chemosensor, 3′,6′-bis(diethylamino)-2-((2,7-dimethoxy-9H-fluoren-9-ylidene)amino)spiro[isoindoline-1,9′-xanthen]-3-one (**1**) for aluminum ion, was designed and synthesized. Compound **1** is an orange colored, weak fluorescent compound which was synthesized via one-step facile reaction of rhodamine B hydrazide with 2,7-dimethoxy-9H-fluoren-9-one in MeOH. When Al^{3+} salt was added in methanol:water (30:70, v/v) solution then spirolactum ring of **1** was opened. The absorbance and fluorescence of the mixed solution were increased dramatically because of the opening of the lactum ring. Thus, signal transduction occurred via reversible CHEF (chelation-enhanced fluorescence) mechanism in the range 580–584 nm.

The design and synthesis of new molecules capable of performing the transduction of fluorescence signal represent a fascinating area of contemporary research related to the detection and quantification of transition metal ions in biological systems and in the environmental remains.[1] After oxygen and silicon, aluminum is the third most abundant (8.3% weight) element in the earth's crust. Due to its importance in many biological and industrial fields, aluminum has been receiving increasing attention. Aluminum is present in its ionic form Al^{3+} in natural waters and biological tissues. The solubility of Al minerals at lower pH increases the amount of available Al^{3+} which is deadly to growing plants and its ultimate effect is the environmental acidification.[2] According to a WHO report, the average daily intake of aluminum is approximately 3–10 mg per day for human beings as it has been widely used in water treatment, as a food additive, aluminum-based pharmaceuticals, and aluminum containers and cooking utensils. Excessive amounts of Al^{3+} can cause a wide range of diseases, such as, Alzheimer's disease, osteoporosis and intoxication in hemodialysis patients. Rickets, gastrointestinal problems, anemia, headaches, decreased liver and kidney function may also be caused by aluminum toxicity.[3] Currently, aluminum detection methods such as, graphite furnace atomic absorption spectrometry and inductively coupled plasma atomic emission spectrometry are relatively complex, expensive and time-consuming in practice. Therefore, the detection of Al^{3+} is highly demanded because of the potential impact of Al^{3+} ions on human health and environment. Now a days, the development of new fluorescent Al^{3+} indicators, especially those that exhibit selective Al^{3+}-amplified emission, is still a challenging job.

Small organic dye molecules have found versatile applications as biomarkers, fluorescent probes, light emitting materials, solar energy harvesting materials etc. Among various options, dye molecules derived from rhodamine, boron dipyrromethane and cyanine moieties are most prominent fluorescent probes because of their long absorption and emission wavelengths within the visible region along with large absorption coefficient and high fluorescence quantum yield.[4] Rhodamine-based fluorescent chemosensors show turn on detection to the targeted heavy transition metal (HTM) cations, such as Pb^{2+}, Cu^{2+}, Hg^{2+}, Fe^{3+}, and Cr^{3+}.[5–8] For example, two rhodamine B molecules were linked through a diethylenetriamine spacer to afford a Fe^{3+} selective sensor.[5a] Xiang et al. reported a rhodamine-based hydrazine bearing a salicylaldehyde binding site as a Cu^{2+} amplified sensor.[5b] Yang et al. reported a Hg^{2+} chemodosimeter based on the rhodamine–hydrazine framework.[5c] In addition, Kwon et al. exploited ethylenediamine to link a rhodamine and a DPA moiety to yield a fluorescent chemosensor for the Pb^{2+} ion.[5d] Spirolactum derivatives of rhodamine dye are useful sensing platforms as the spirolactum ring-opening process leads to a turn on fluorescence change. Addition of metal cation leads to a spirocyclic ring-opening which is accompanied by a vivid color change from colorless to pink, thus enabling detection simple with the 'bare eye'.

Our group has some interest in the synthesis of chemosensors in general and Al^{3+} in particular. Accordingly, herein we report for the first time a new rhodamine-based spirolactam derivative (**1**) as a

* Corresponding author. Tel.: +91 33 24322936; fax: +91 33 23519755.
E-mail address: skkar_cu@yahoo.co.in (S.K. Kar).

0040-4039/$ - see front matter © 2013 Elsevier Ltd. All rights reserved.
http://dx.doi.org/10.1016/j.tetlet.2013.04.103

chemosensor for Al^{3+},[9–13] where binding phenomena could be probed through binding-induced changes in an electronic spectral pattern. To the best of our knowledge, no such example is there in literature. Further, binding of this metal ion to **1** caused a drastic color change, which could also be detected by the 'naked eye' under UV light. Interestingly, binding of only Al^{3+} to **1** caused significant fluorescence enhancement in an aqueous-methanol mixture. In this mixed solvent medium, the chemosensor **1** demonstrated Al^{3+}-specific emission enhancement through a 1:1 (**1**+Al^{3+}) binding mode with the metal ion. Rhodamine B hydrazide was synthesized following a literature procedure and characterized by ^1H NMR spectra FT-IR and mass data.[14,5b] It was then condensed with 2,7-dimethoxy-9H-fluoren-9-one in methanol to form **1** in 75% yield (Scheme 1). The structure of compound **1** was confirmed by its spectroscopic and analytical data (^1H NMR, FT-IR, HRMS, see Supplementary data S1–S3).

UV–vis spectrum recorded for **1** (70 μM) in MeOH using HEPES buffer [50 μM, MeOH:water = 3:7 (v/v), pH ~ 7] at 25 °C exhibited absorption peak at 545 nm. This absorption band was generated predominantly due to intraligand π–π* charge transfer transition. However, upon gradual addition of Al^{3+} ions (2.5 μM) at a time up to 100 μM caused a gradual increase in intensity with concomitant shift of the band to 560 nm ($\varepsilon = 2.3 \times 10^2\ M^{-1}\ cm^{-1}$) along with a color change from colorless to deep pink at this concentration. Therefore, there was a large enhancement of absorbance. The formation of a new band at 560 nm occurred due to the opening of the spirolactum ring of the rhodamine moiety. This absorption peak was expected on account of coordination of **1** with Al^{3+}. This phenomenon illustrated the transformation of free **1** to the Al^{3+}-coordinated species. So the chemosensor **1** can indeed serve as a highly sensitive 'naked eye' indicator for Al^{3+} (Fig. 1). However, upon the addition of various other biologically important metal ions, such as perchlorates of Na^+, Mg^{2+}, Pd^{2+}, Hg^{2+}, Ni^{2+}, Co^{2+}, Cd^{2+}, Zn^{2+}, and Pb^{2+}, up to 100 μM had no significant effect on absorption properties of chemosensor **1**. A mild increase of absorbance at 550 nm was also detected upon addition of the same amount (100 μM) of Cu^{2+} solution. Upon addition of Fe^{3+} to **1**, a red shift occurred and absorbance increased at 555 nm (Fig. 2). In case of Fe^{3+} and Cu^{2+}, this enhancement in absorbance clearly suggests the formation of the delocalized xanthane moiety of the rhodamine group associated with pale pink color change. A bright orange fluorescence was observed only for (**1**+Al^{3+}) solution, and no fluorescence for other metal cations under UV-light (366 nm) was recorded (Fig. 3). This was an interesting feature by which we could detect Al^{3+} exclusively without any other instrumental technique.

The fluorescence property of **1** (15 μM) was investigated in MeOH using HEPES buffer [50 μM, MeOH:water = 3:7 (v/v), pH ~ 7] at 25 °C, (λ_{ex} = 545 nm) (Fig. 4). Without cations, **1** showed a very weak fluorescence peak at 563 nm which was probably because of the trace open ring molecules of **1** in solution state. However, upon gradual addition of Al^{3+} (2.5 μM) at a time to a 15 μM solution of **1** in MeOH at 25 °C (with HEPES buffer, pH ~ 7), showed distinct behavior with quenching of emission intensity at 563 nm and the appearance of a new peak at 584 nm. This red shift (~21 nm) was accompanied by enhanced fluorescence intensity. A turn-on ratio over 15-fold was triggered with the addition 0–70 equiv of Al^{3+}. The enhancement of the fluorescence intensity

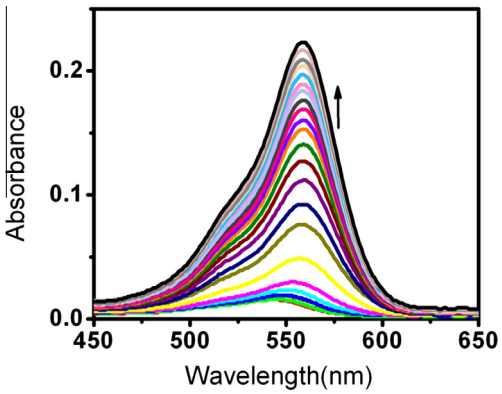

Figure 1. UV–vis absorption spectra of chemosensor **1** (70 μM) with increasing amounts of $Al_2(SO_4)_3{\cdot}16H_2O$ (total of 100 μM) in MeOH using HEPES buffer [50 μM, MeOH:water = 3:7 (v/v), pH ~ 7] at 25 °C.

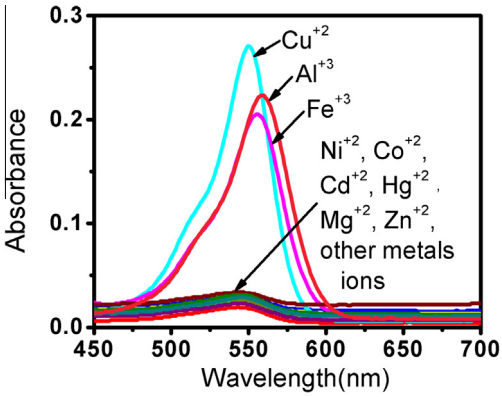

Figure 2. UV–vis spectra of receptor **1** (70 μM) with addition of perchlorate salts of Al^{3+}, Na^+, Mg^{2+}, Pd^{2+}, Hg^{2+}, Ni^{2+}, Co^{2+}, Cd^{2+}, Zn^{2+}, and Pb^{2+} (a total of 100 μM) in MeOH using HEPES buffer [50 μM, MeOH:water = 3:7 (v/v), pH ~ 7] at 25 °C.

was due to the formation of a (**1**+Al^{3+}) complex, which resulted in the selective CHEF effect. The association constant (K_a)[15] of **1** with Al^{3+} was $3 \times 10^7\ M^{-1}$, as obtained by nonlinear least-squares analysis (Figs. S4 and S6 in the Supplementary data). Al^{3+} could be detected at least down to be 2.4×10^{-6} M by fluorimetric assay, indicating that the limit of detection of **1** to Al^{3+} met the limit for drinking water. The fluorescence quantum yields[16] (Φ_{fs}) of compound **1** in the free and Al^{3+}-bound state were found to be 0.07 and 0.43, respectively. Stoichiometry for the (**1**+Al^{3+}) complex with respect to Al^{3+} and ligand was evaluated on the basis of the Job's plot[17] and result confirmed the formation of 1:1 complex (Fig. S5 in the Supplementary data). We also tested the fluorescence response of **1** to other metal ions such as Ag^+, Ca^{2+}, Zn^{2+}, Ni^{2+}, Co^{2+}, Mg^{2+}, Na^+, and K^+ (100 μM) in aqueous-MeOH media at pH ~ 7 (Fig. 5 and Fig. S7 in the Supplementary data). Only Fe^{3+} responded towards slight increase in fluorescence intensity at 577 nm, while other metal ions did not show any significant change under identical conditions. Al^{3+} has ionic radius of 0.57 Å, whereas that of Fe^{3+} is 0.67 Å, as the Fe^{3+} has greater ionic radius compared to that

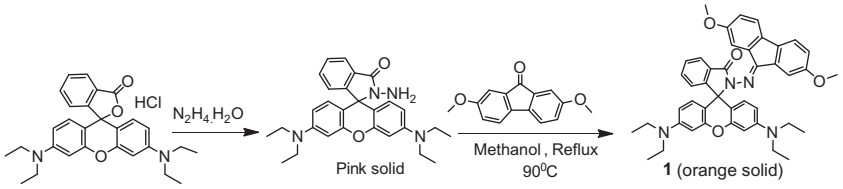

Scheme 1. Synthesis of chemosensor **1**.

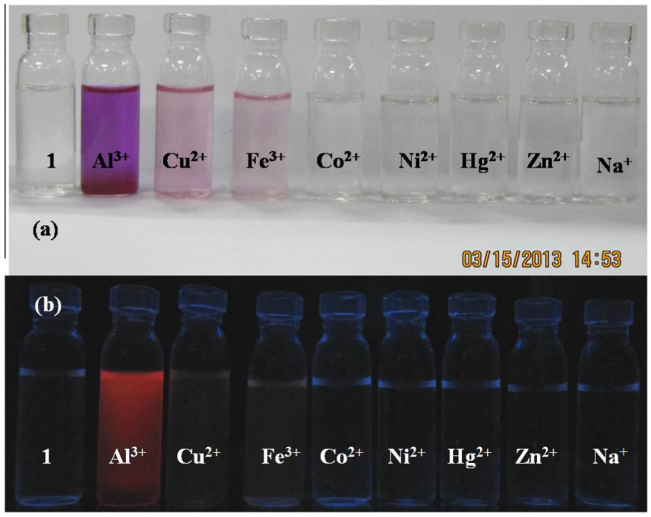

Figure 3. Photographs of chemosensor **1** (70 μM) with different metal ions (100 μM) in MeOH using HEPES buffer [50 μM, MeOH:water = 3:7 (v/v), pH ~ 7] at 25 °C under (a) visible light and (b) UV light.

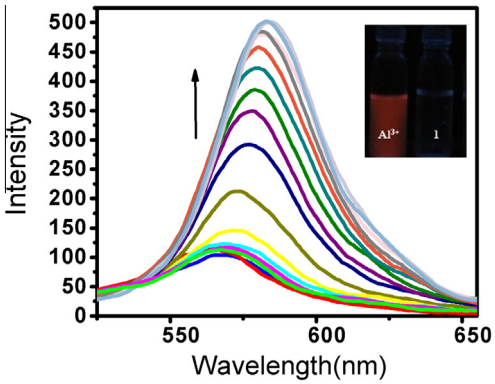

Figure 4. Fluorescent titration spectra of **1** (15 μM) in MeOH using HEPES buffer [50 μM, MeOH:water = 3:7 (v/v), pH ~ 7] at 25 °C (λ_{ex} = 545 nm) in the presence of different concentrations of $Al_2(SO_4)_3{\cdot}16H_2O$. Inset: fluorescence intensity at 584 nm as a function of Al^{3+} concentration and showing the fluorescence of **1** and the addition of Al^{3+} ions.

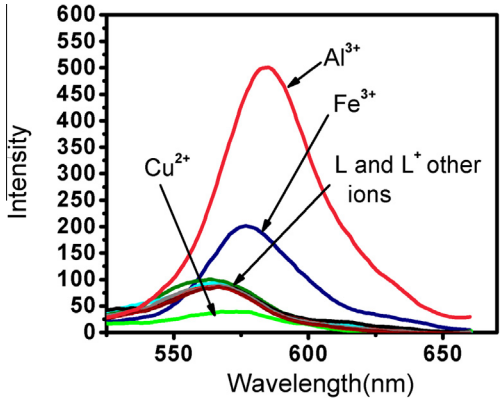

Figure 5. Fluorescence spectra (excitation at 545 nm) of **1** (15 μM) with addition of perchlorate salts of Al^{3+}, Na^+, Mg^{2+}, Pd^{2+}, Hg^{2+}, Ni^{2+}, Co^{2+}, Cd^{2+}, Zn^{2+}, and Pb^{2+} (a total of 100 μM) in MeOH using HEPES buffer [50 μM, MeOH:water = 3:7 (v/v), pH ~ 7] at 25 °C.

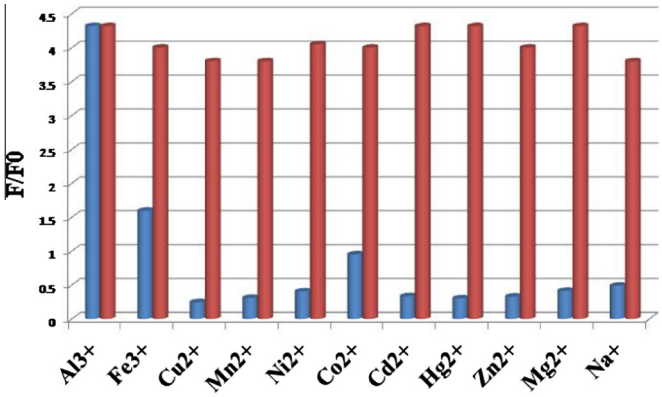

Figure 6. Fluorescence response of **1** (15 μM) to various cations (100 μM) in MeOH using HEPES buffer (50 μM, MeOH: water = 3:7 (v/v), pH ~ 7] at 25 °C (λ_{ex} = 545 nm). Bars represent the emission intensity ratio F/F_0 (F_0 = initial fluorescence intensity at 584 nm; F = final fluorescence intensity at 584 nm after the addition of Al^{3+} ions). The blue bars represent the addition of individual metal ions while the red bars represent the change in the emission that occurs upon the subsequent addition of Al^{3+} (100 μM) to the above solution.

of Al^{3+}. Therefore, it could not fit well into the sterically crowded coordination zone of the rhodamine-based Schiff based ligand. We carried out competitive experiments in the presence of 100 μM Al^{3+} along with 100 μM other cations such as Zn^{2+}, Ni^{2+}, Co^{2+}, Mg^{2+}, Na^+, Cu^{2+}, Hg^{2+}, Cd^{2+}, Fe^{3+}, and Mn^{2+}. There was no significant variation in the fluorescence emission of the solution of (**1**+Al^{3+}) when the measurement is carried out with or without the other metal ions (Fig. 6). However, the addition of same amount of (100 μM) Cu^{2+}, the fluorescence intensity of the chemosensor **1** was quenched to a great extent. The fluorescence quenching occurred mainly due to the excitation energy transfer from the ligand to the metal d-orbital and/or ligand to metal charge transfer (LMCT) in aqueous-methanol medium.[18] Thus, the selectivity observed for Al^{3+} over other metal ions was remarkably high. This unique selectivity of **1** towards Al^{3+} could be interpreted in terms of the smaller ionic radii (0.57 Å) and higher charge density (r = 4.81) of the Al^{3+} ion. The smaller radii of the Al^{3+} ion permit suitable coordination geometry of the chelating chemosensor **1** and the larger charge density allows a strong coordination ability between **1** and Al^{3+}.[19] As the metal ions Al^{3+} binds strongly with the ligand, the possible flexible modes which are responsible for nonradiative decay are hindered and hence fluorescence intensity enhancement was observed. Reversible binding of **1** with Al^{3+} was also examined. Addition of total (0–100 μM) of Na_2EDTA to a mixture of **1** and Al^{3+} resulted in diminution of the fluorescence intensity at 584 nm which signifies the regeneration of spirolactum structure (Fig. S8 in the Supplementary data). Such reversibility and regeneration were important for the fabrication of devices to sense the Al^{3+} ions. As pH dependence of fluorescence is generally undesirable in biological applications, the effect of pH on fluorescence was also studied in aqueous-methanol. It was found that

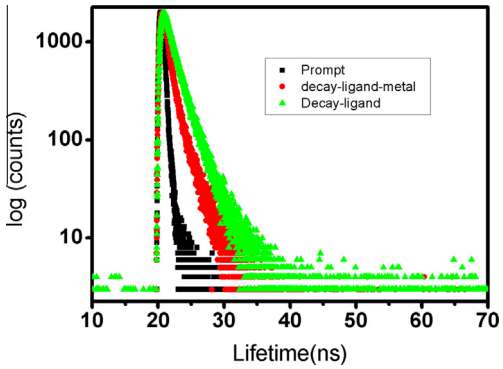

Figure 7. Time-resolved fluorescence decay of **1** (green)+Al^{3+} (red).

the fluorescence intensity of free **1** at 584 nm remained unchanged over a wide pH range 4.5–14 (Fig. S9 in the Supplementary data), whereas the addition of the Al^{3+} ion could lead to a remarkable increase of fluorescence, due to efficient complexation between **1** and Al^{3+} ion. These results indicated that **1** could be used as a selective fluorescent probe to recognize Al^{3+} in the presence of various interfering metal ions.

This was further confirmed by time correlated single photon-counting (TCSPC) studies using a 340 nm LED as an excitation source. It had been used to examine the excited state behavior of the free chemosensor **1** and its metal complex in aqueous-MeOH (Fig. 7). According to the equations[20] $\tau^{-1} = k_r + k_{nr}$ and $k_r = \Phi_f/\tau$, the radiative rate constant k_r and the total nonradiative rate constant k_{nr} of **1** and Al^{3+}-bound species were calculated. The fluorescence decay curves for the chemosensor **1** and its metal complex were fitted by bi-exponential function with acceptable χ^2 values and all the data were presented in (Table S1 in the Supplementary data). The data suggested that the factor that induced fluorescent enhancement was mainly due to the more than 100 times increase of k_r. This enhancement was attributed to the introduction of Al^{3+} and the strong complexation occurring with **1**, as was evident from the large binding constant value.

^{1}H NMR titration in DMSO-d_6 was carried out in order to clarify the binding mechanism of Al^{3+} with receptor **1** (Fig. 8). Addition of 1 equiv of Al^{3+} resulted no change of any chemical shifts. High-resolution mass spectra (HRMS) also provided additional evidence for the formation of a 1:1 complex between Al^{3+} ion and **1** (Fig. 9). Further it was clearly observed that upon addition of the Al^{3+} ion, the carbonyl stretching band of **1** at 1699 cm^{-1} was changed to a lower wave number (1685 cm^{-1}). Both ^{1}H NMR, mass and IR results firmly support that the carbonyl group of spirolactum is involved in the Al^{3+} binding, thus inducing a ring-opening of the spirolactum in **1**.

In conclusion, we have synthesized a unique chromogenic and fluorogenic Al^{3+} probe using rhodamine derivative as a fluorophore. The mechanism for rhodamine-based sensors depends on the Al^{3+} induced ring-opening reaction of a rhodamine spirolactum scaffold compared with reported Al^{3+} fluorescent probe. The proposed probe exhibits the following advantages: a quick, simple and facile synthesis. Furthermore, the solution of **1** itself a weak fluorescent and colorless ('clear blank'); thus greater fluorescence enhancement and remarkable color change toward Al^{3+} can be achieved. Under UV light illumination, one can visually detect even 5 ppm Al^{3+} in aqueous buffer solution without the aid of any sophisticated instruments. Thus the chemosensor **1** was able to serve as a 'naked eye' chemodosimeter for Al^{3+}, allowing its reversible detection in the presence of a wide range of environmentally relevant competing metals ions.

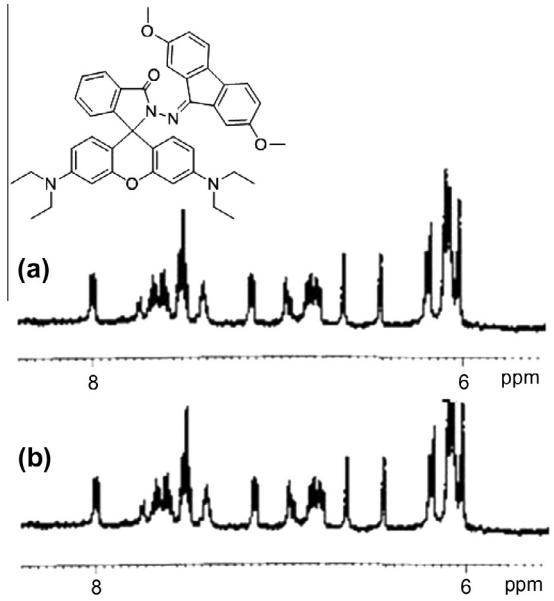

Figure 8. ^{1}H NMR tritration of **1** and with Al^{3+} ion (DMSO-d_6). (a) **1** only (b) **1** with 1 equiv of Al^{3+}.

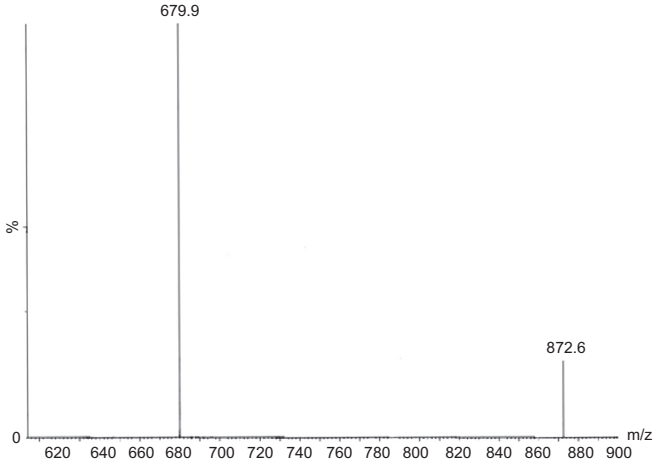

Figure 9. HRMS spectra of **1**+Al^{3+} complex. The peak at m/z = 872.6 was assigned to the derivative of **1**·$Al(SO_4)$·$3H_2O$·(OH).

Acknowledgments

A.J. thanks CSIR for award of senior research fellowship. This work is also supported by the Council of Scientific and Industrial Research (CSIR), New Delhi, India (Project No. 01(2401)/10/EMR-II).

Supplementary data

Supplementary data (supplementary figures and table) associated with this article can be found, in the online version, at http://dx.doi.org/10.1016/j.tetlet.2013.04.103.

References and notes

1. (a) de Silva, A. P.; Gunaratne, H. Q. N.; Gunnlaugsson, T.; Huxley, A. J. M.; McCoy, C. P.; Rademacher, J. T.; Rice, T. E. *Chem. Rev.* **1997**, *97*, 1515–1566; (b) Callan, J. F.; de Silva, A. P.; Magri, D. C. *Tetrahedron* **2005**, *61*, 8551–8588; (c) Pina, E.; Bernardo, M. A.; Garcia-Espana, E. *Eur. J. Inorg. Chem.* **2000**, 2143–2157; (d) Valeur, B.; Leray, I. *Acc. Chem. Res.* **2000**, *205*, 3–40; (e) Rurack, K.; Resch-Genger, U. *Chem. Soc. Rev.* **2002**, *31*, 116–127.
2. (a) Barcelo, J.; Poschenrieder, C. *Environ. Exp. Bot.* **2002**, *48*, 75–92; (b) Rogers, M. A. M.; Simon, D. G. *Age Ageing* **1999**, *28*, 205; (c) Krejpcio, Z.; Wojciak, R. W. *Pol. J. Environ. Stud.* **2002**, *11*, 251; (d) Flaten, T. P.; Ødegard, M. *Food Chem. Toxicol.* **1988**, *26*, 959–960; (e) Ren, J.; Tian, H. *Sensors* **2007**, *7*, 3166–3178; (f) Yokel, R. A. *Neurotoxicology* **2000**, *21*, 813–828.
3. (a) Fasman, G. D. *Coord. Chem. Rev.* **1996**, *149*, 125; (b) Nayak, P. *Environ. Res.* **2002**, *89*, 111; (c) Cronan, C. S.; Walker, W. J.; Bloom, P. R. *Nature* **1986**, *324*, 140; (d) Berthon, G. *Coord. Chem. Rev.* **2002**, *228*, 319; (e) Burwen, D. R.; Olsen, S. M.; Bland, L. A.; Arduino, M. J.; Reid, M. H.; Jarvis, W. R. *Kidney Int.* **1995**, *48*, 469.
4. Kim, H.; Lee, M.; Kim, H.; Kim, J.; Yoon, J. *Chem. Soc. Rev.* **2008**, *37*, 1465–1472.
5. (a) Xiang, Y.; Tong, A. *Org. Lett.* **2006**, *8*, 1549; (b) Xiang, Y.; Tong, A.; Jin, P.; Ju, Y. *Org. Lett.* **2006**, *8*, 2863; (c) Yang, Y.-K.; Yook, K.-J.; Tae, J. *J. Am. Chem. Soc.* **2005**, *127*, 16760; (d) Kwon, J. Y.; Jang, Y. J.; Lee, Y. J.; Kim, K. M.; Seo, M. S.; Nam, W.; Yoon, J. *J. Am. Chem. Soc.* **2005**, *127*, 10107.
6. Rode, B. A.; Kim, J.; Kim, H. S.; Gupta, G.; Hong, S. I. *Tetrahedron Lett.* **2012**, *53*, 2571–2574.
7. Yu, C.; Wang, T.; Xu, K.; Zhao, J.; Li, M.; Weng, S.; Zhang, J. *Dyes and Pigments* **2013**, *96*, 38–44.
8. Song, C.; Zhang, X.; Jia, C.; Zhou, P.; Quan, X.; Duan, C. *Talanta* **2010**, *81*, 643–649.

9. Maity, D.; Govindaraju, T. *Inorg. Chem.* **2010**, *49*, 7229–7231.
10. Maity, D.; Govindaraju, T. *Chem. Commun.* **2010**, 4499–4501.
11. Ren, J. L.; Zhang, J.; Luo, J. Q.; Pei, X. K.; Jiang, Z. X. *Analyst* **2001**, *126*, 698–702.
12. Wang, Y.-W.; Yu, M.-X.; Yu, Y.-H.; Bai, Z.-P.; Shen, Z.; Li, F.-Y.; You, X.-Z. *Tetrahedron Lett.* **2009**, *50*, 6169–6172.
13. Kim, S. H.; Choi, H. S.; Kim, J.; Lee, S. J.; Quang, D. T.; Kim, J. S. *Org. Lett.* **2010**, *12*, 560–563.
14. Anthoni, U.; Christophersen, C.; Nielsen, P.; Puschl, A.; Schaumburg, K. *Struct. Chem.* **1995**, *3*, 161–165.
15. Connors, K. A. *Binding Constants*; Wiley: New York, 1987.
16. (a) Teuchner, K.; Pfarrherr, A.; Stiel, H.; Freyer, W.; Leupold, D. *Photochem. Photobiol.* **1993**, *57*, 465–471; (b) Freyer, W.; Dahne, S.; Minh, L. Q.; Teuchner, K. *Z. Chem.* **1986**, *26*, 334–336; (c) Stiel, H.; Teuchner, K.; Paul, A.; Freyer, W.; Leupold, D. *J. Photochem. Photobiol., A* **1994**, *80*, 289–298.
17. Vosburgh, W. C.; Copper, G. R. *J. Am. Chem. Soc.* **1941**, *63*, 437–442.
18. Dalapati, S.; Jana, S.; Alam, M. A.; Guchhait, N. *Sensor. Actuat. B: Chem.* **2011**, *60*, 1106–1111.
19. Chen, C. H.; Liao, D. J.; Wan, C. F.; Wu, A. T. *Analyst* **2013**, *138*, 2527–2530.
20. Saha, U. C.; Chattopadhyay, B.; Dhara, K.; Mandal, S. K.; Sarkar, S.; Khuda-Bukhsh, A. R.; Mukherjee, M.; Helliwell, M.; Chattopadhyay, P. *Inorg. Chem.* **2011**, *50*, 1213–1219.